Exploring the effect of the Herschel-Quincke duct combined with a micro-perforated duct for enhanced sound attenuation

Kael H. Cadete, Wanderson V. O. Monteiro, José M. C. Dos Santos

Dept. of Computational Mecanics, University of Campinas Rua Mendeleyev, 200, Cidade Universitária, Campinas-SP, Brazil.
k205974@dac.unicamp.br, w203198@dac.unicamp.br, zema@unicamp.br,

Abstract. This present study evaluates the effectiveness of a periodic acoustic metamaterial system comprised of Herschel-Quincke (H-Q) ducts for noise control. The methodology employed is based on a transfer matrix (TM) approach. The results regarding sound transmission loss are validated through finite element simulations carried out in the Comsol multiphysics software. Furthermore, the Floquet-Bloch theory is utilized to identify bandgaps in infinite periodic silencers, highlighting the frequency ranges where sound waves are significantly attenuated. Additionally, several Herschel-Quincke tube models are proposed, incorporating variations in the number and shape of H-Q tubes. This results in defining structural parameters that exhibit substantial improvements in their sound attenuation capabilities, particularly in expanding the frequency range where attenuation occurs.

Keywords: Herschel-Quincke, Metamaterials, Transfer Matrix, Sound Transmission Loss

1 Introduction

Acoustic filters have been studied over the past few decades, [1] evaluated the duct configuration known as the Herschel-Quincke (HQ) filter, which consists of a main duct and a parallel duct (called the HQ duct) that is of a different length than the main duct. When an acoustic wave propagates within the duct, a phase shift occurs between the wave traveling in the main duct and the wave traveling in the HQ duct, resulting in destructive interference of the acoustic waves when they meet, at certain frequencies.

The acoustic attenuation of the HQ duct occurs within specific frequency ranges, which consequently become narrow, similar to the effect of local resonance. Due to this, various models have been proposed to enhance its efficiency in attenuating acoustic waves [2–4].

One way to improve the narrow attenuation range of HQ ducts is by coupling them with other systems. For example, [5] used a micro-perforated chamber muffler (MPCM) coupled with an HQ duct to passively control the axial noise of a fan. In this study, various configurations of the HQ duct coupled with an MPCM were evaluated, and a transfer matrix (TM) was formulated based on the equations governing acoustic systems. The results were validated using the finite element method (FEM) with the Comsol Multiphysics software.

2 Transfer Matrix Formulation

In this section, the Transfer Matrix modeling for the acoustic ducts, HQ resonator, MPCM and its combinations are reviwed and presented. The classical Herschel-Quincke duct model is combined with a MPCM. By locally modeling the tranfer matrices and the continuity of pressure acoustic and particle velocity, the final structural model is achieved.

2.1 Modeling MPCM

The micro-perforated region of the duct is inside of an expansion chamber, that has the same length (L_c) of the MPCM region, it can be seen in Figure 1.

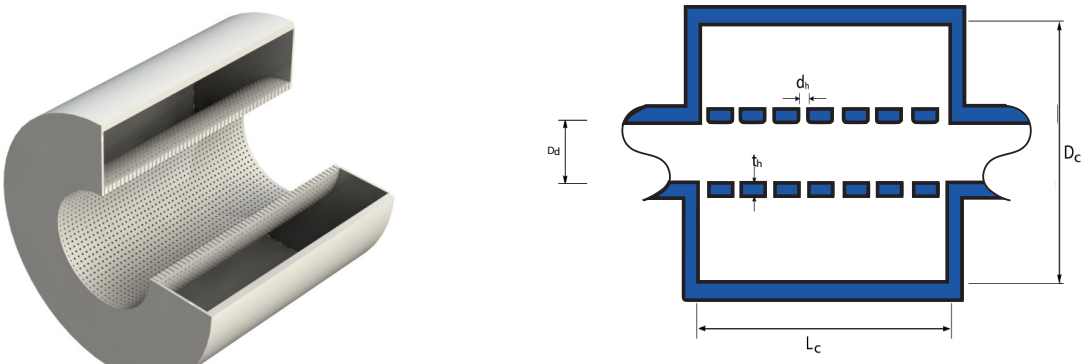

(a) Isometric view of the MPCM.

(b) Schematic of the MPCM parameters.

Figure 1. Representation of a MPCM duct with an expansion chamber.

Considering that only plane waves propagate thought the duct, and the pressure at the inlet and outlet of the MPCM are $\{p_2 \;\; p_2^{'}\}$ and the mass velocity $\{v_2 \;\; v_2^{'}\}$, the equations that govern the system are [6]:

$$\begin{aligned} &\frac{d^2p_2}{dx^2} + \left(k^2 - j\frac{4k}{D_d z}\right)p_2 + j\frac{4k}{D_i z}p_2^{'} = 0 \\ &\frac{d^2p_2^{'}}{dx^2} + j\frac{4D_d k}{(D_c^2 - D_d^2)z}kp_2 + \left(k^2 - j\frac{4D_d}{(D_c^2 - D_d^2)z}k\right)p_2^{'} = 0, \end{aligned} \tag{1}$$

in which D_c and D_d are the expansion chamber and the MPCM ,respectively, k is the wave number and z is the specific acoustic impedance of the MPCM duct, given by [7]

$$z = \frac{32\eta t_h}{\sigma\rho c d_h^2}\left[\sqrt{1+\frac{K^2}{32}} + \frac{\sqrt{2}}{32}K\frac{d_h}{t_h}\right] + j\frac{\omega t_h}{\sigma c}\left[1 + \frac{1}{\sqrt{9+\frac{K^2}{2}}} + 0.85\frac{d_h}{t_h}\right], \tag{2}$$

in this context, $K = d_h\sqrt{\omega\rho/4\eta}$, η is the air viscosity, ρ is the air mass density, c is the sound velocity, d_h the diameter of the MPCM, t_h the wall thickness, $\sigma = N_f A_f/A_l$ is the porosity, where N_f is the number of holes, A_f is the area of the hole and A_l is the duct surface area.

Acoustic pressure and mass velocity can be related by $dp/dx = -jkYv$, using the relationship, transformed the Eqn.1 1 in state space formulation :

$$\frac{d}{dx}\begin{Bmatrix} p_2 \\ -v_2 \\ p_2^{'} \\ -v_2^{'} \end{Bmatrix} = \underbrace{\begin{bmatrix} 0 & jkY_1 & 0 & 0 \\ \frac{4}{D_i z Y_1} + j\frac{k}{Y_1} & 0 & -\frac{4}{D_i z Y_1} & 0 \\ 0 & 0 & 0 & jkY_2 \\ -\frac{4D_i}{(D_c^2 - D_i^2)zY_2} & 0 & \frac{4D_i}{(D_c^2 - D_i^2)zY_2} + j\frac{k}{Y_2} & 0 \end{bmatrix}}_{\mathbf{G}} \begin{Bmatrix} p_2 \\ -v_2 \\ p_2^{'} \\ -v_2^{'} \end{Bmatrix}, \tag{3}$$

wherein Y_1 and Y_2 are the characteristic impedance of the duct with the diameter D_i and D_c, respectively. In one-dimensional systems with length L, the input and output can be related by transfer matrix, give by:

$$\mathbf{y}(L) = \mathbf{T}_G\mathbf{y}(0), \tag{4}$$

at which $\mathbf{T}_G = e^{\mathbf{G}L}$. A computationally efficient way to calculate this matrix is through the eigenvectors ($\mathbf{\Psi}$) and eigenvalues (λ), of the form $\mathbf{T}_G = \mathbf{\Psi}e^{\lambda L}\mathbf{\Psi}^{-1}$. Since the wall is rigid, we have the mass velocity around it ($v_2^{'}(0) = 0$) and ($v_2^{'}(L) = 0$), it can be reduced to:

$$\mathbf{T}_m = \begin{bmatrix} T_{G_{11}} - \frac{T_{G_{13}}T_{G_{41}}}{T_{G_{43}}} & T_{G_{12}} - \frac{T_{G_{13}}T_{G_{42}}}{T_{G_{43}}} \\ T_{G_{21}} - \frac{T_{G_{23}}T_{G_{41}}}{T_{G_{43}}} & T_{G_{22}} - \frac{T_{G_{23}}T_{G_{42}}}{T_{G_{43}}} \end{bmatrix}. \tag{5}$$

where $\mathbf{T}_m$ is the MPCM transfer matrix.

2.2 Modeling HQ resonator with MPCM

The transfer matrix of a circular tube can be written by [8]

$$\mathbf{T}_d = \begin{bmatrix} cos(kl) & iYsin(kl) \\ i\frac{sin(kl)}{Y} & cos(kl) \end{bmatrix}, \tag{6}$$

where l is the tube length, $Y = \rho c/S$ is the characteristic impedance with S as the cross-sectional area.

The upper tube in the HQ (B branch) is called the resonator, and the lower tube (A branch) which is called the main duct. Figure 2 shows the Herschel-Quincke resonator (B branch), including an MPCM in the A branch.

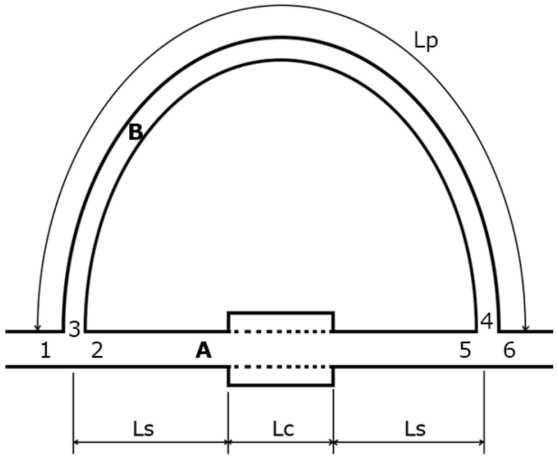

Figure 2. Herschel-Quincke resonator including an MPCM in A branch.

The waves propagating from the states (1) split between (2) and (3). The waves coming from the state (3) travel through the resonator (B branch) going to (4), and the waves coming from the state (2) travel through the ducts and MPCM (A branch) going to (5). The waves from the states (5) and (4) meet at (6). It can be seen that the pressure in the bifurcations is equal to $p_1 = p_2 = p_3$ and $p_4 = p_5 = p_6$. By the continuity, the volume velocity of the states is related by $v_1 = v_2 + v_3$ and $v_4 + v_5 = v_6$. The resonator is a circular duct with the transfer matrix given by Eq. (6), the relationship between the states (3)-(4) is given by,

$$\begin{Bmatrix} p_3 \\ v_3 \end{Bmatrix} = \mathbf{T}_B \begin{Bmatrix} p_4 \\ v_4 \end{Bmatrix}, \tag{7}$$

where $\mathbf{T}_B = \mathbf{T}_d$. The main duct now includes a duct before the MPCM, the MPCM itself, and a duct after MPCM. Since the elements are in series the transfer matrix can be written as $\mathbf{T}_A = \mathbf{T}_{in}\mathbf{T}_m\mathbf{T}_{out}$, and the relationship between the states (2)-(5) is given by,

$$\begin{Bmatrix} p_2 \\ v_2 \end{Bmatrix} = \mathbf{T}_A \begin{Bmatrix} p_5 \\ v_5 \end{Bmatrix} \tag{8}$$

where $\mathbf{T}_{in} = \mathbf{T}_{out} = \mathbf{T}_d$. From the compatibility conditions and the Eqs. (7) and (8), it's possible to obtain,

$$\mathbf{T}\mathbf{p_o} = \mathbf{p_i} \tag{9}$$

where $\mathbf{T}$ is the system transfer matrix, $\mathbf{p_o} = \{p_6\ v_6\ p_2\ v_2\ p_3\ v_3\ p_4\ v_4\ p_5\ v_5\}^T$ is the output state vector and $\mathbf{p_i} = \{p_1\ 0\ 0\ 0\ v_1\ 0\ 0\ 0\ 0\ 0\}^T$ is the input state vector. Rearranging the Eq. (9), the transfer martix of the system can be rewritten as:

$$\begin{Bmatrix} p_6 \\ v_6 \end{Bmatrix} = \begin{bmatrix} \mathbf{T}^{-1}(1,1) & \mathbf{T}^{-1}(1,5) \\ \mathbf{T}^{-1}(2,1) & \mathbf{T}^{-1}(2,5) \end{bmatrix} \begin{Bmatrix} p_1 \\ v_1 \end{Bmatrix}. \tag{10}$$

From the transfer matrix of the system, it's possible to find the sound transmission loss of the system by [8]

$$STL = 20\log_{10}\left|\sqrt{\frac{Y_{in}}{4Y_{out}}}\left(\mathbf{T}(1,1)+\frac{\mathbf{T}(2,1)}{Y_{out}}+\mathbf{T}(1,2)Y_{in}+\mathbf{T}(2,2)\frac{Y_{in}}{Y_{out}}\right)\right|. \tag{11}$$

where Y_{in} and Y_{out} are the characteristics impedance of the inlet and outlet of the system, respectively.

The transfer matrix of the system ($\mathbf{T}$) can relate the state on the right ($\mathbf{q}_R$) with the state on left ($\mathbf{q}_L$) by:

$$\mathbf{q}_L = \mathbf{T}\mathbf{q}_R. \tag{12}$$

By considering the system as a unit-cell of an infinity periodic system, then for m consecutive unit-cells, the Eq. (12) can be rewritten as:

$$\mathbf{q}_L^{(m+1)} = \mathbf{T}\mathbf{q}_R^{m}, \tag{13}$$

The volume velocity and acoustic pressure compatibility and continuity condition between unit-cells produces $\mathbf{q}_R^{(m)} = \mathbf{q}_L^{(m+1)}$, by substituting in the Eq.(13) it has:

$$\mathbf{q}_L^{(m+1)} = \mathbf{T}\mathbf{q}_L^{m+1}, \tag{14}$$

Abandoning the superscript of Eq. (14) and applying the Floquet-Bloch theorem, it has,

$$\mathbf{q}_L = e^{\mu}\mathbf{q}_L, \tag{15}$$

where $\mu = -ikL_c$ is the constant of attenuation, k is the wavenumber, and L_c is the unit-cell length. Substituting Eq. (12) in the Eq. (15) and abandoning the subscripts, produces:

$$\mathbf{T}\mathbf{q} = e^{\mu}\mathbf{q}, \tag{16}$$

or

$$\left(\mathbf{T} - \mathbf{I}e^{\mu}\right)\mathbf{q} = \mathbf{0}, \tag{17}$$

which is the Bloch wave eigenproblem, where e^{μ} are the eigenvalues or the Bloch wavenumbers, $\mathbf{q}$ are the corresponding eigenvectors or Bloch waves vectors, and $\mathbf{I}$ is the identity matrix. The dispersion diagram ($f \times k$) can be obtained from the Bloch wavenumbers, and the bandgaps can be identified.

3 Simulated Results

The results of the analyzed system were made using the transfer matrix method (TM) in MatLab software and verified by the finite element method (FEM) in COMSOL Multiphysics software.

The validation of Herschel-Quincke and the MPCM models was performed separately. The HQ resonator dimensions are $L_p = 0.8m$, $d_p = 0.04m$, $L_d = 0.4m$, and $d_d = 0.05m$. Figure 3(a) shows STL results for the HQ model calculated by TM and FEM. It can be observed that there is a very good agreement between methods. The MPCM dimensions are $t_h = 3mm$, $D_c = 50mm$, $D_d = 150mm$, $d_h = 0.8mm$, and $N_f = 400$ holes. Figure 3(b) shows the STL results for the MPCM model calculated by TM and FEM, where it can be seen a very good agreement between methods. These results verify the TM computation code.

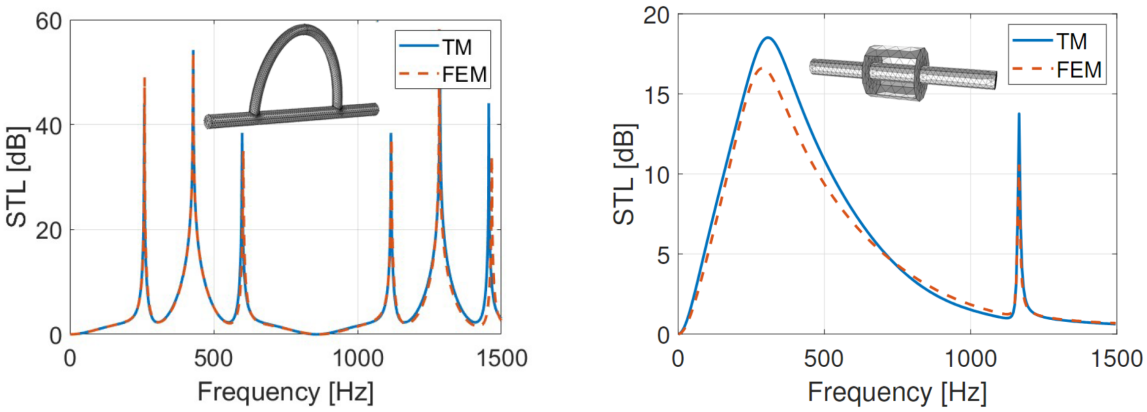

(a) HQ resonator STLs calculated by TM and FEM methods.

(b) MPCM STLs calculated by TM and FEM methods.

Figure 3. Validation of HQ resonator and MPCM models by TM and FEM methods.

Combining the HQ resonator (HQ) with the microperforated chamber muffler (MPCM), two new acoustic filters are proposed. One consists of including an MPCM in the A branch (MPCM+HQ-A) of the HQ resonator (Fig. 2), and the other includes an MPCM in the B branch (MPCM+HQ-B) of the HQ resonator. To evaluate the performance of MPCM+HQ combinations, the STL results calculated by TM for the HQ, MPCM, and MPCM+HQ-A and -B are compared.

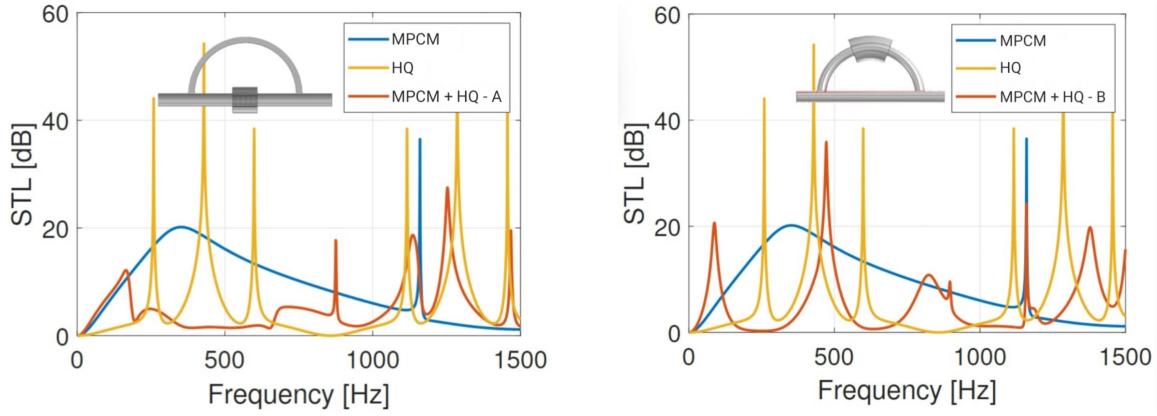

(a) STL calculated by TM for HQ, MPCM and MPCM+PC-A. (b) STL calculated by TM for HQ, MPCM and MPCM+PC-B.

Figure 4. STL comparison between HQ, MPCM and MPCM+HQ-A and -B.

Figure 4(a) shows the STLs calculated by TM for the HQ, MPCM, and MPCM+HQ-A. It can be seen that the STL performance of MPCM+HQ-A is inferior to that of HQ and MPCM, mainly at a low-frequency range (about 200-1200 Hz). For higher-frequency bands (1.2-1.5 kHz) the MPCM presents inferior performance than MPCM+HQ-A and HQ. Figure 4(b) shows the STLs calculated by TM for the HQ, MPCM, and MPCM+HQ-B. It can be seen that for some frequency ranges (about 0-100, 300-600, 700-900 Hz), the MPCM+HQ-B model presents superior STL performance than HQ and MPCM. Also, these frequency bands happen where the HQ and MPCM present very low STL performances. These results indicate that this promising combination (MPCM+HQ-B model) should be further explored.

Another filter is proposed, which consists of an in-series connection (MPCM+HQ-S) of one HQ resonator (HQ) with one microperforated chamber muffler (MPCM). Figure 5 shows the STLs calculated by TM for the

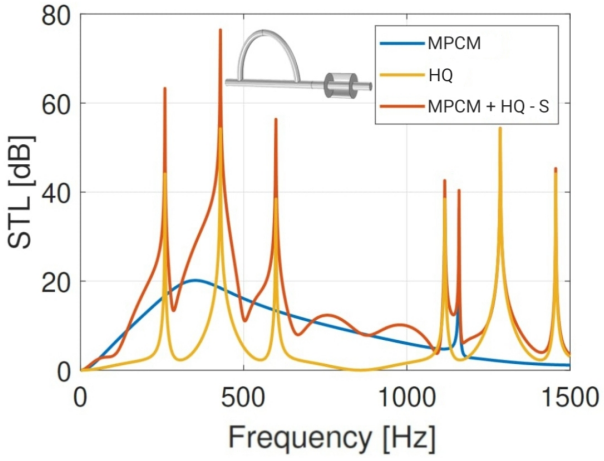

Figure 5. STL comparison between HQ, MPCM, and MPCM+HQ in-series.

HQ, MPCM, and MPCM+HQ-S. As expected, it can be seen that this combination of HQ resonator in-series with MPCM presents the best attenuation of the cases studied. This configuration is better than the resonator isolated since the filtering effect in-series is added.

Using HQ resonator and MPCM this acoustic filtering concept is extended to consider a periodic acoustic metamaterial with a unit-cell as a MPCM+HQ-S. Figure 6(b) shows the dispersion diagram for the metamaterial with a unit-cell MPCM+HQ-S. It can be seen that some bandgap formations ($\Im(kL) \neq 0$) are due to local resonance (negative acute peaks) and periodicity Bragg effect (negative smooth peaks). These results indicate that by

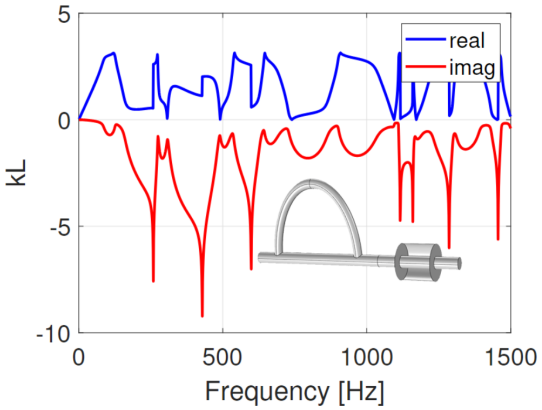

(a) Dispersion Diagram.

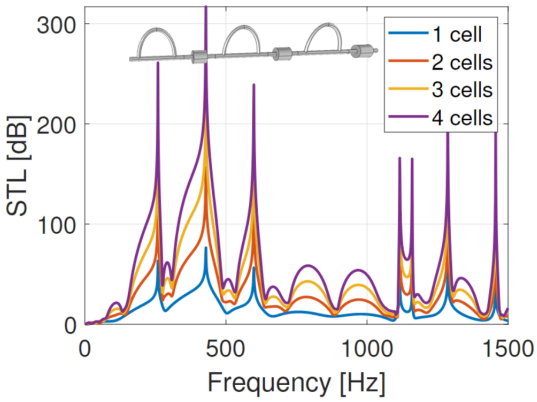

(b) STLs calculated by TM for the metamaterial with $N = 1, 2, 3, 4$ unit-cells.

Figure 6. Acoustic periodic metamaterial with a unit-cell MPCM+HQ-S.

using these acoustic devices in the right configuration, efficient metamaterials can be designed. Figure 6 shows the STL performance of the metamaterial varying the number of unit-cells cells (N). As expected, as the number of cells increases the STL performance of metamaterial improves.

4 Conclusions

In the present work, the Herschel-Quincke (HQ) resonator combined with a multiperforated chamber muffler (MPCM) in multiple spatial configurations is evaluated. The paper reviews the transfer matrix (TM) method to model the HQ and MPCM acoustic devices to find the sound transmission loss (STL) of coupled systems. Furthermore, the computational implementation of the TM method is validated using the finite element method of COMSOL Multiphysics software.

Combining the HQ resonator with the microperforated chamber muffler (MPCM) included in the A branch of the HQ resonator, its STL performance is inferior to that of HQ and MPCM at a low-frequency range, while for higher-frequency bands the MPCM is inferior to the MPCM+HQ-A and HQ. The other configuration, which includes the MPCM in the B branch of the HQ resonator, the STLs performance for some frequency ranges presents superior STL performance than HQ and MPCM, and these frequency bands happen where the HQ and MPCM present very low STL performances. These results indicate that this promising combination should be further explored.

Another filter is proposed, which consists of an in-series connection (MPCM+HQ-S) of one HQ resonator (HQ) with one microperforated chamber muffler (MPCM). As expected, this combination of HQ in-series with MPCM presents the best attenuation of the cases studied since the filtering effect in-series is added, and the results will be better than the resonators alone.

Using an HQ resonator and MPCM, this acoustic filtering concept is extended to consider a periodic acoustic metamaterial with a unit-cell as an MPCM+HQ in-series. The results show that some bandgap formations are obtained due to local resonance and periodicity. Results indicate that by using acoustic devices in the right configuration, efficient metamaterials can be designed. As expected, as the number of cells in metamaterial increases, the STL performance of metamaterial improves. Of course, these are preliminary results and more research needs to be made and are underway.

Acknowledgements. The authors are grateful to the financial support of the Brazilian research funding, FAPESP (Grant No. 15894-0/2018, Grant No. 12112-0/2023) , and CNPq (Grant No. 317436/2021-0).

Authorship statement. The authors hereby confirm that they are the sole liable persons responsible for the authorship of this work, and that all material that has been herein included as part of the present paper is either the property (and authorship) of the authors, or has the permission of the owners to be included here.

References

[1] G. W. Stewart. The theory of the herschel-quincke tube. *Phys. Rev.*, vol. 31, pp. 696–698, 1928.
[2] R. Siqueira Mazzaro, S. de Morais Hanriot, R. Jorge Amorim, and P. Américo Almeida Magalhães Júnior. Numerical analysis of the air flow in internal combustion engine intake ducts using herschel-quincke tubes. *Applied Acoustics*, vol. 165, pp. 107310, 2020.
[3] H. Ahmadian, G. Najafi, B. Ghobadian, S. Reza Hassan-Beygi, and R. J. Bastiaans. Analytical and numerical modeling, sensitivity analysis, and multi-objective optimization of the acoustic performance of the herschel-quincke tube. *Applied Acoustics*, vol. 180, pp. 108096, 2021.
[4] P. Theodosios, E. Tsolakis, V. Spitas, and A. Movchan. The herschel-quincke tube with modulated branches. *Philosophical Transactions of the Royal Society A: Mathematical, Physical and Engineering Sciences*, vol. 380, 2022.
[5] Z. Wang, Y. Chiang, Y. Choy, C. Wang, and Q. Xi. Noise control for a dipole sound source using micro-perforated panel housing integrated with a herschel–quincke tube. *Applied Acoustics*, vol. 148, pp. 202–211, 2019.
[6] A. Selamet, I. Lee, and N. Huff. Acoustic attenuation of hybrid silencers. *Journal of Sound and Vibration*, vol. 262, pp. 509–527, 2003.
[7] D.-Y. Maa. Theory and design of microperforated panel sound-absorbing constructions. *Scientia Sinica*, vol. 18, n. 1, pp. 54–71, 1975.
[8] M. L. Munjal. *Acoustics of ducts and mufflers*. John Wiley e Sons Inc, New York, 2014.